Precision Agric (2011) 12:775–794
DOI 10.1007/s11119-011-9220-y

# Using apparent soil electrical conductivity ($EC_a$) to characterize vineyard soils of high clay content

**José Ramon Rodríguez-Pérez · Richard E. Plant · Jean-Jacques Lambert · David R. Smart**

Published online: 18 February 2011


**Abstract** The adoption of precision viticulture requires a detailed knowledge of variation in soil chemical, physical and profile properties. This study evaluates the usefulness of apparent electrical conductivity ($EC_a$) data within a GIS framework to identify variations in soil chemical and physical properties and moisture content. The work was conducted in a vineyard located in the Carneros Region (Napa Valley, California). The soil was sampled using 44 boreholes to quantify chemical and physical characteristics and 9 open pits to verify the borehole observations. Moisture content was determined using time domain reflectometry (TDR). To characterize soil $EC_a$, three campaigns were undertaken using a soil electrical conductivity meter (EM38). Linear regressions between soil $EC_a$ and soil properties were determined. Boreholes and TDR data were interpolated by kriging to characterize the spatial distribution of soil variables. The resulting maps were compared to the results obtained using the best $EC_a$ linear regressions. Using $EC_a$ measurements, soil properties like extractable $Na^+$ and $Mg^{2+}$, clay and sand content were well estimated, while best estimates were obtained for extractable $Na^+$ ($r^2 = 0.770$) and clay content ($r^2 = 0.621$). The best estimates for soil moisture content corresponded to moisture in the deeper soil horizons ($r^2 = 0.449$). The methods described above provided maps of soil properties estimated by $EC_a$ in a GIS framework, and could save time and resources during vineyard establishment and management.

**Keywords** Apparent electrical conductivity · GIS · Spatial interpolation · Precision viticulture · Soil spatial variation

J. R. Rodríguez-Pérez
Geomatics Engineering Research Group, Universidad de León, Avenida de Astorga, s/n, 24400 Ponferrada, Leon, Spain

R. E. Plant
Department of Plant Sciences, University of California, One Shields Avenue, Davis, CA 95616, USA

J.-J. Lambert · D. R. Smart (✉)
Department of Viticulture and Enology, University of California, Robert Mondavi Institute N, 595 Hilgard Lane, Davis, CA 95616, USA
e-mail: drsmart@ucdavis.edu

## Introduction

The apparent electrical conductivity of the vadose zone ($EC_a$) is most strongly dependent on soil moisture content and solution electrolyte concentration. Nonetheless $EC_a$ can be influenced by a host of physical and chemical factors in addition to moisture content and salt concentration. These other properties include porosity, clay content and its mineralogy, temperature and phase of water retained in pores (Corwin and Lesch 2005). The composition of soil colloids, depth to clay-rich layers, depth to groundwater and root density can also influence $EC_a$ measurements (McNeill 1980a).

The use of soil $EC_a$ has gained attention as a good surrogate method for detection of spatial variation in the chemical and physical properties of intact soils and to map such factors. Irrigation drainage patterns (Corwin and Lesch 2005), compaction (Hedley et al. 2004) and sand and clay content (Domsch and Giebel 2004) are examples of such physical properties. Soil $EC_a$ is the most extensively used method for estimating soil salinity in tilled soil under irrigation (De Clercq and Van Meirvenne 2005; Horney et al. 2005). In addition, soil $EC_a$ has been used in agricultural settings to characterize a number of soil properties besides salinity that have an influence on plant performance. Such applications that have been found useful include estimation of fertility, organic material and the volumetric water content ($\theta_v$) (Hedley et al. 2004). This is largely possible because $\theta_v$ is the other dominant factor in addition to the true electrical conductivity ($EC_e$—which is a function of electrolyte concentration) that is detected in a natural soil when measuring $EC_a$ (Noborio 2001; Shmulik 2005). Fertility generally corresponds to availability of ions of the principal plant macro- and micronutrients. A number of recent scientific reviews exist concerning the use of $EC_a$ to estimate soil properties (Allred et al. 2008; Corwin and Lesch 2005; Hendrickx et al. 2002).

There exist a number of procedures for measuring soil $EC_a$ at the field scale. A primary method is electromagnetic induction (McNeill 1980b). The use of this procedure has several advantages relative to other methods that use electrodes: excellent resolution of conductivity is generally achieved, problems associated with soil penetration are avoided and the ease and speed with which numerous measurements can be gathered in the field is greatly increased (McNeill 1980b).

The most commonly used electromagnetic induction conductivity meter for agricultural purposes is the EM38 (Geonics Limited, Mississauga, Ontario, Canada) because of ease of use and a functional measurement depth (Corwin and Lesch 2005). The EM38 can be placed in the horizontal coil configuration, where its effective signal detection ($\pm$70% of the response) is from 0.75 m, or in the vertical coil configuration with an effective signal detection depth of 1.5 m (Geonics Limited 1999). These depths generally correspond well with the depth of the grape rooting zone (Smart et al. 2006).

In viticulture, the measurement of $EC_a$ to estimate edaphic parameters that condition vineyard productivity is in its infancy. As with other agricultural crops, the most extensively studied application concerns the assessment of salinity of vineyards in grape production primarily in Australia (Bramley and Lanyon 2002; Bramley 2004; Bramley and Hamilton 2004) as well as long-term effects of irrigation (De Clercq and Van Meirvenne 2005). Soil $EC_a$ has also been used to map soil texture in viticulture areas of France (Winkel et al. 1995) and New Zealand (Hedley et al. 2004). Acevedo-Opazo et al. (2008) used soil electrical properties (electrical resistivity), vine information (vegetative, water status and harvest) and airborne imagery to estimate soil water content so that vine water restriction within vineyards could be defined. The most extensive current applications are related to precision viticulture because $EC_a$ has been found to estimate spatial patterns of grape yield (Bramley 2003). Yield spatial heterogeneity forms a strong basis for developing site-specific practices in most agricultural crops but in viticulture crop loads are often managed and quality parameters take precedence. Nevertheless, protocols for the mapping of $EC_a$ in vineyards as a tool in the application of precision viticulture (Williams and Bramley 2003), center on exploiting the advantages of the method for explaining the spatial variability of soil moisture, fertility and texture, which are related to yield. One factor which differs from many annual crops is that grape root systems can explore several soil horizons and to depths that may sometimes exceed that of the sensing capabilities of the EM38 (Smart et al. 2006).

The objectives of this study were (1) to assess the effectiveness of apparent electrical conductivity as a surrogate in the measurement of soil properties of high clay vineyard soils (clay content >25%) such as those found in the Coastal Regions of California, and (2) to develop regression models that might be used to predict soil properties based on measured $EC_a$. The EM38 was used, positioning the instrument in both the horizontal and vertical modes of dipole orientation for the estimation of soil $EC_a$. The data obtained were then correlated with the weighted mean averages of soil chemical and physical variables and moisture from boreholes extracted to the effective rooting depth of the soil. To accomplish this, three field data collection campaigns were carried out on different dates, each of which had different air temperatures and soil moisture conditions. This approach allowed the conditions to be identified under which soil $EC_a$ would effectively estimate horizontal changes in soil chemical and physical properties deemed important to vine performance.

## Materials and methods

### Location

The work was conducted in a 3.66 ha vineyard located in the Carneros Region of the Napa Valley (CA, USA). The study location is shown in Fig. 1, and lies within the co-ordinates SW (38.247104°N, 122.3663210°W) and NE (38.247982°N, 122.361995°W) (WGS1984). The vineyard was planted in 1991 with *Vitis vinifera* cv. Pinot Noir clone UC 2A with a 1.5 m × 2.4 m vine by row spacing. The trellis/training system consisted of unilateral cordons trained to vertical shoot positioning (VSP) on a two-wire trellis system that was 2 m in height. The rootstock was *V. rupestris* × *V. riparia* cv. 3309C.

### Soil chemical and physical properties

The vineyard was sampled in 2003 to characterize soil chemical and physical properties. The lower slopes soils of the vineyard consisted of Haire Clay Loam series (fine, mixed, superactive, thermic Typic Haploxerult) while on the upper slopes the soils were Diablo Clay series (fine, montmorillonitic, superactive, thermic Typic Pelloxerert). Forty-four boreholes were used for physical and chemical analyses and twelve open soils pits were established to determine bulk densities and verify the major soil horizons observed for a total of 56 observations. The boreholes were laid out in a grid pattern of 8.5 m NS by 24.5 m EW to correspond with 300 data vines (20 rows with 15 data vines per row) that were slightly offset by the irregularity of the vine rows. The open pits were established paying attention to slope heterogeneity in the vineyard. Three soil pits were established on the shoulder of the slope, two sets of three were in the midslope region, and three were in the toe-slope. Nine of the twelve pits were analyzed for chemical and physical properties as

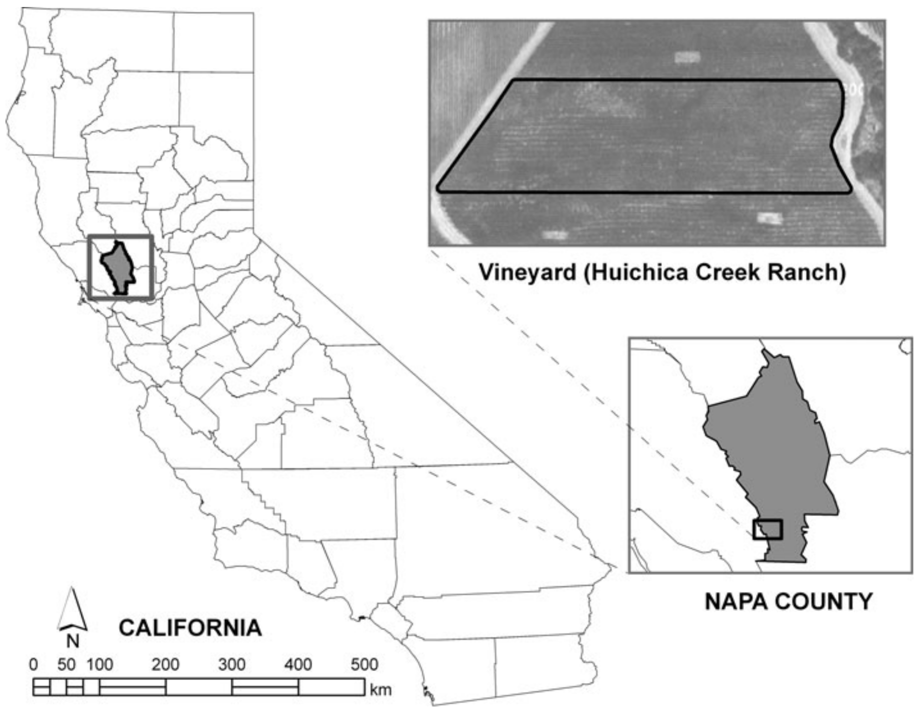


**Fig. 1** Location of the study area in the Carneros, Napa Co., California USA

described below for the borehole samples and were reported by Steenwerth et al. (2008). After these positions had been established, a Trimble Ag 132 backpack DGPS receiver (Trimble Navigation Inc. Sunnyvale, CA, USA) with sub-meter post processing accuracy was used to determine the geographic location of each pit and borehole.

The pits had the dimensions of 0.6 m width by 2.0–2.5 m depth and were 4 m in length. One wall of each pit was established at approximately 0.25 m away from the vine rows. Morphological designations were assigned to each horizon. The soil depth intervals sampled (1–4 depths in 9 of 12 pits) was 0–0.36, 0.36–0.70, 0.70–1.04 and 1.04–1.38 m, respectively. Soil depth 1, the surface depth, represented the Ap horizon (0–0.36 m). Soil depth 2 (0.36–0.70 m) corresponded to the beginning of the next subtending horizon and included morphological designations over the total vineyard area of A, BAt, Bt1, AC, and, in one case, C1. Soil depth 3 (0.70–1.04) was positioned below soil depth 2 and included Bt1, Bt2, C1, C2, and 2C2. Soil depth 4, the deepest sampled area at 1.04–1.38 m, corresponded to the deeper depths detected by the EM38, and included Bt2, BCt, C1 and C2 horizons. These designations and consolidations were selected because extensive terraforming occurred at this site during 1992 prior to planting (Smart et al. 2008). Geospatial redistribution of the vadose zone soils in order to mitigate undesirable slopes resulted in the inversion or otherwise removal of natural soil horizonation. Thus, the above groupings and use of depth-directed sampling of soils proved necessary.

Bulk density at each depth was measured using metal brass rings that were 60 mm in depth with a volume of $3.32 \times 10^5$ mm$^3$. Soils were dried at 105°C for 48 h and used to calculate gravimetric water content (GWC). Air-dry soil samples were sieved at 2 mm. The 0–2 mm fraction was analyzed for exchangeable cations (x-K, x-Na, x-Ca, x-Mg; see

Thomas 1982), cation exchange capacity (CEC), pH by the saturated paste method (US Salinity Lab Staff 1954), total carbon (C) and nitrogen (N) by Dumas combustion (Pella 1990), and particle-size distribution (i.e., sand, silt and clay) according to Gee and Bauder (1986). All soil analyses were conducted by the Department of Agriculture and Natural Resources Analytical Laboratory (URL: danranlab.ucdavis.edu).

### Soil moisture content

Soil water content in situ was determined using a time domain reflectometry (TDR) system (Topp et al. 1980). The primary components of the TDR system (Environmental Sensors Inc., ESI, Victoria, BC, Canada) were an analog-to-digital converter and datalogger (ESI model MP-917) and a 0.9 m TDR waveguide (ESI model PRB-F). The PRB-F waveguide is partitioned into segments that measure at depths of 0–0.15 m, 0.15–0.30 m, 0.30–0.45 m, 0.45–0.60 m and 0.60–0.90 m. Recommended protocols (ESI 2002) were used for both calibration of the instrument and field data collection with it. Prior to its use, the PRB-F waveguide was calibrated in the laboratory by inserting it into a microcosm cylinder (0.40 cm diameter × 1.50 m depth) filled with fine sand and insuring that each segment reported the same moisture content at field capacity (FC, $\theta_v = 12\%$). In the field, $\theta_v$ estimates from the PRB-F were verified by inserting it into the soil to a depth of 0.90 m and gathering measurements from all segments. Then a 5.5 cm diameter by 0.90 m depth soil core was taken ($n = 4$) using a manual tool (Giddings, Windsor, CO, USA). At each depth corresponding to the PRB-F segments, approximately 50 g moist soil (sieved to pass a 2 mm mesh) was sub-sampled and dried in an oven at 104°C to determine gravimetric water content according to the method of Gardner (1986). The gravimetric water content ($\theta_g$) was converted to $\theta_v$ using the soil bulk density (Mg $m^{-3}$) and a specific mass for water of 1 (Mg $m^{-3}$). No significant differences were detected and the measured values were within the reported accuracy of TDR technologies of 3%.

The soil moisture content campaigns were undertaken on July 7th and 8th, 2005. The position and number of points sampled were taken at locations corresponding to those of the borehole samples taken in 2003 (soil sampling campaign described above). The TDR system was used to determine $\theta_v$ parallel to locations and within 0.5 m of the 44 boreholes.

### Apparent soil electrical conductivity

Measurements of soil $EC_a$ were collected using an EM38 soil electrical conductivity meter. Three EM38 campaigns were undertaken on July 8th, July 29th and September 19th, 2005. The EM38 instrument was calibrated before each measurement following Geonics Limited (1999) instructions. Measurements of soil $EC_a$ were made at 150 locations corresponding to alternating rows of the 150 paired and geo-referenced data vines. Included within these data positions were the 44 locations where boreholes had been established in 2003 for soil chemical and physical analyses. Thus, six data sets of $EC_a$ were obtained: three in horizontal dipole orientation $EC_a$1h, $EC_a$2h and $EC_a$3h, and three in vertical dipole orientation $EC_a$1v, $EC_a$2v and $EC_a$3v, collected on July 8th, July 29th and September 19th, respectively. When a sample was collected at a borehole location, the EM38 was positioned at approximately 1.5 m N offset, parallel with the row orientation and $EC_a$ data were gathered in both dipole orientations.

It has recently been reported that trellis systems can cause substantial interference with EM38 measurements when metal stakes are used with a full complement of foliage and drip irrigation support wires, and the EM38 is positioned close to it (Lamb et al. 2005). The vineyard trellis system consisted of wooden stakes and a limited number of foliage support wires (3). Several independent tests of the EM38 by our group indicated that no such interference existed when the EM38 was positioned in the center of the alley, thus maximizing its distance from the trellis (see Lamb et al. 2005). This was done by placing the EM38 in the center of the alley and taking a reading, and then moving it progressively closer to, and parallel to, the wooden posts of the vine row. The EM38 measurement did not change appreciably (<10%) when moved to the proximity of the posts (see Lamb et al. 2005, who generally noted less than a 20% increase of the signal in the center of the row when metal trellis stakes were used).

## Data pre-processing and statistical analyses

Samples of soil taken from the 44 boreholes corresponded to visible soil horizons observed in the open pits, and therefore were taken at variable depths. For this investigation, the soil samples were weighted at each of the borehole positions by assigning a general value for soil chemical and physical properties to each location according to the following:

$$x_m = \frac{\sum x_i \cdot d_i}{D} \tag{1}$$

where $x_m$ is the weighted mean average, $x_i$ is the analytical value observed for the depth sub-sample $i$, $d_i$ is the depth of the observed sub-sample $i$, and $D$ is the total depth of the borehole. This approach may not be valid if large differences are observed in soil chemical and physical properties with depth, or if differences are noted in $EC_a$h versus $EC_a$v. However, neither of these situations were observed in the measurements.

To determine which soil characteristics most strongly influenced $EC_a$h and $EC_a$v, the Pearson Product Moment Correlations ($r$) were computed for measurements made at the borehole locations. Data pairs that were most strongly correlated were then subjected to linear regression analysis as described below. Statistical analyses were undertaken using the SPSS Statistics v.13.0 (SPSS Inc., Chicago, Illinois USA).

A general linear test (Bates and Watts 1988) was used to assess whether the linear relationships were different among different measurement dates and sampling positions. This method involves the fitting of full and reduced models and has frequently been applied to assess whether separate models are necessary for different data sets. The full model corresponds to different sets of global parameters for different measurement dates/sampling positions and is obtained by expanding the two parameters of the linear model by including an associated parameter and a dummy variable to differentiate the measurement date and the position of the sample. The dummy variable is a categorical variable which can only take the values of 0 or 1. The reduced model corresponds to the same set of global parameters for all measurements analyzed. For example, for the linear function:

$$Soil\,Clay\,Content = a + b \cdot EC_a \tag{2}$$

The expansion of the slope parameter b for the three measurement dates and the two sampling positions can be written as:

$$b_1 + b_2 \cdot I_2 + b_3 \cdot I_3 + b_4 \cdot I_4 + b_5 \cdot I_5 + b_6 \cdot I_6 \tag{3}$$

where $b_i (i = 1, 2, \ldots, 6)$ are the associated parameters of the full model, and $I_j (j = 2, \ldots, 6)$ are the categorical variables for considering the six different measurements (three dates and two positions), which are defined as follows:

$I_2 = 1$ if measurement date = July 8th in horizontal position, otherwise $I_2 = 0$;
$I_3 = 1$ if measurement date = July 29th in vertical position, otherwise $I_3 = 0$;
$I_4 = 1$ if measurement date = July 29th in horizontal position, otherwise $I_4 = 0$;
$I_5 = 1$ if measurement date = September 19th in vertical position, otherwise $I_5 = 0$;
$I_6 = 1$ if measurement date = September 19th in horizontal position, otherwise $I_6 = 0$.

The appropriate test statistic uses the following expression:

$$F = \frac{SSE_R - SSE_F}{df_R - df_F} \div \frac{SSE_F}{df_F} \quad (4)$$

where $SSE_R$ is the error sum of squares of the reduced model, $SSE_F$ is the error sum of squares of the full model, and $df_R$ and $df_F$ are the degrees of freedom of the full and reduced models, respectively. Under the standard linear regression assumptions the statistic defined in Eq. 4 follows an $F$-distribution. It was not attempted to correct for possible spatial autocorrelation of errors. Preliminary analysis (not shown) indicated that spatial autocorrelation did not materially affect the analysis.

If the $F$-test indicates that no statistically significant differences exist in the linear models between the different dates and EM38 orientations, then one may aggregate all of the sample data into a single model. If the $F$-test indicates that significant differences exist, accepting as significant a value of $p \leq 0.05$, further tests are necessary to evaluate whether or not the differences were caused by a few or many of the possible combinations of factors sampled at each location. For this report, the regressions for each edaphic factor were obtained for $EC_a$v and $EC_a$h for each $EC_a$ campaign. It was further tested whether or not differences existed among the soil chemical and physical properties on each sampling date, and it did not.

### Spatial distribution of soil factors

Interpolated thematic maps were generated for the measured soil parameters from the 44 borehole and 9 analyzed pit sample locations using the geostatistical module contained in ArcGIS v. 9.1 (ESRI, Redlands, CA, USA), interpolating according to the ordinary kriging model. The number of borehole samples is generally considered much too low a number for accurate kriging interpolation, so these comparisons must be considered qualitative and informal only. Nevertheless, they do provide a general indication of the patterns of distribution of the various soil components. Maps were constructed for each estimated variable using the best-fit regression equations for $EC_a$v and $EC_a$h. The resulting map resolution was 2.5 m per pixel. This exercise was also realized using the Map Calculator module of ArcGIS v. 9.1.

## Results and discussion

### Chemical and physical soil properties

Table 1 presents overall summary statistics for soil samples taken from nine soils pits at the site at four overall depths. As expected, soil carbon and nitrogen contents significantly declined with depth. For particle size distribution (sand, silt, clay) and extractable cation contents, no significant differences existed with the exception of extractable sodium ($Na^+$) content. The quantities of exchangeable cations observed, including sodium, indicated no

**Table 1** Means, standard errors and mean separation for soil characteristics ($n = 9$)

| Soil characteristic | Soil depth 1 (0–0.36 m) | Soil depth 2 (0.36–0.70 m) | Soil depth 3 (0.70–1.04 m) | Soil depth 4 (1.04–1.38 m) |
|---|---|---|---|---|
| Sand (%) | 45.0 ± 4.1a | 48.0 ± 6.2a | 48.1 ± 8.6a | 45.3 ± 8.5a |
| Silt (%) | 25.8 ± 2.3a | 22.8 ± 3.1a | 20.0 ± 3.8a | 23.1 ± 4.1a |
| Clay (%) | 29.2 ± 2.9a | 29.2 ± 4.0a | 31.9 ± 5.1a | 31.6 ± 5.2a |
| pH | 6.4 ± 0.2a | 6.7 ± 0.3a | 7.0 ± 0.4a | 7.2 ± 0.4a |
| CEC* (cmol $kg^{-1}$ soil) | 28.3 ± 2.6a | 26.7 ± 3.3a | 29.0 ± 4.2a | 30.1 ± 3.7a |
| x-K (cmol $kg^{-1}$) | 0.4 ± 0.0a | 0.3 ± 0.0b | 0.3 ± 0.0b | 0.3 ± 0.0b |
| x-Ca (cmol $kg^{-1}$) | 12.8 ± 1.3a | 12.3 ± 1.4a | 13.0 ± 1.5a | 16.1 ± 2.5a |
| x-Mg (cmol $kg^{-1}$) | 6.6 ± 1.2a | 7.6 ± 1.6ab | 9.5 ± 2.0ab | 10.2 ± 2.0b |
| x-Na (cmol $kg^{-1}$) | 0.2 ± 0.0a | 0.4 ± 0.1ab | 1.0 ± 0.3bc | 1.5 ± 0.5c |
| Total N (g $kg^{-1}$) | 1.10 ± 0.06a | 0.70 ± 0.08b | 0.48 ± 0.04c | 0.42 ± 0.02c |
| Total C (g $kg^{-1}$) | 10.32 ± 0.83a | 5.2 ± 1.1b | 2.46 ± 0.48c | 2.47 ± 0.60c |
| Bulk density (g/$cm^3$) | 1.24 ± 0.06a | 1.38 ± 0.05b | 1.47 ± 0.07b | 1.44 ± 0.06b |

*Lower letters* indicate significant differences by ANOVA using Bonferroni's mean separation test with a probability of committing a Type I Error of $p \leq 0.05$. CEC is cation exchange capacity

**Table 2** Extractable concentrations (meq 100 $g^{-1}$) of the base cations of $K^+$, $Na^+$, $Ca^{2+}$ and $Mg^{2+}$

| | $K^{+a}$ | $Na^{+a}$ | $Ca^{2+a}$ | $Mg^{2+a}$ | Clay[b] | Silt[b] | Sand[b] |
|---|---|---|---|---|---|---|---|
| Maximum | 1.26 | 2.78 | 20.71 | 16.29 | 43.7 | 34.7 | 71.5 |
| Minimum | 0.15 | 0.02 | 7.72 | 3.74 | 13.8 | 14.7 | 23.8 |
| Mean | 0.35 | 0.70 | 13.32 | 8.83 | 30.3 | 25.7 | 44.0 |
| Median | 0.35 | 0.53 | 12.75 | 8.84 | 31.6 | 25.3 | 42.2 |
| SD | 0.16 | 0.58 | 2.93 | 2.91 | 7.3 | 5.4 | 11.5 |
| CV | 0.45 | 0.82 | 0.22 | 0.33 | 0.24 | 0.21 | 0.26 |

Soil particle size distributions (%) for soils sampled at 44, 2 m boreholes ($n = 44$) in a Pinot Noir vineyard in the Carneros Region, Napa Valley California USA

Method of analysis: [a] Thomas 1982; [b] Sheldrick and Wang 1993

general problems with salinity at this site. The values weighted for the total depth of the boreholes (Eq. 1) agreed well with the observations from the open pits (Table 2). Tests for normality indicated that the soils data generally followed normal distributions (Table 2) and therefore were appropriate for conducting correlation analyses against $EC_a$ and for mapping exercises using geostatistical methods. Coefficients of variation (CV) were generally less than 30% but in a few cases, most notably $Na^+$, CVs greatly exceeded that level.

## Relationship between $EC_a$ and soil moisture content

The descriptive statistics for the soil $\theta_v$ campaign are shown in Table 3. Substantial variation was noted in moisture content, but this was attributed almost entirely to soils with either very high sand contents (lower $\theta_v$) or very high clay contents (higher $\theta_v$), as expected. Descriptive statistics for the $EC_a$ measurements are given in Table 4. Substantial variation among the $EC_a$ measurements over the vineyard also existed. The most elevated

**Table 3** Volumetric soil moisture content $\theta_v$ (%) measured on July 7–8th 2005

| | Depth (m) | | | | | Profile (0–0.90 m) | |
|---|---|---|---|---|---|---|---|
| | 0–0.15 | 0.15–0.30 | 0.30–0.45 | 0.45–0.60 | 0.60–0.90 | Mean | Weighted average |
| Maximum | 29.8 | 36.5 | 28.0 | 35.0 | 57.4 | 30.6 | 34.5 |
| Minimum | 4.1 | 4.0 | 2.2 | 8.4 | 15.0 | 10.0 | 10.8 |
| Mean | 15.4 | 19.5 | 16.7 | 22.4 | 37.1 | 22.2 | 24.7 |
| Median | 14.3 | 19.2 | 16.6 | 23.5 | 36.8 | 22.5 | 25.4 |
| SD | 6.3 | 6.9 | 5.8 | 6.5 | 10.9 | 4.8 | 5.6 |
| CV | 0.41 | 0.35 | 0.35 | 0.29 | 0.29 | 0.22 | 0.22 |

Shown are the means for all depths sampled, and the weighted average (Eq. 1) inasmuch as each sample depth was different

**Table 4** $EC_a$ (mS $m^{-1}$) data set collected during three field campaigns in 2005: (July 8th, July 29th and September 19th, 2005) for horizontal ($EC_a1h$, $EC_a2h$ and $EC_a3h$) and vertical ($EC_a1v$, $EC_a2v$ and $EC_a3v$) dipole orientations

| | July 8th | | July 29th | | September 19th | |
|---|---|---|---|---|---|---|
| | Horizontal ($EC_a1h$) | Vertical ($EC_a1v$) | Horizontal ($EC_a2h$) | Vertical ($EC_a2v$) | Horizontal ($EC_a3h$) | Vertical ($EC_a3v$) |
| Maximum | 68.00 | 96.75 | 52.00 | 81.00 | 52.25 | 73.37 |
| Minimum | 18.63 | 19.00 | 15.00 | 21.00 | 17.87 | 15.63 |
| Mean | 42.69 | 52.36 | 32.52 | 46.79 | 32.35 | 37.47 |
| Median | 43.75 | 54.50 | 31.00 | 46.00 | 30.94 | 34.63 |
| SD | 11.75 | 18.71 | 9.32 | 14.41 | 8.76 | 14.00 |
| CV | 0.28 | 0.36 | 0.28 | 0.31 | 0.27 | 0.37 |

absolute values were acquired during the campaign of July 8th when the EM38 was held in the vertical dipole orientation and the lowest readings were obtained on the campaign of September 19th when soils were drier.

The *r* values were calculated between EM38 measurements in both dipole orientations and the soil volumetric water content ($\theta_v$) as determined for each soil depth interval using the TDR soil profiling system. The correlation coefficients for each soil depth interval are shown in Table 5. The correlation coefficients for $\theta_v$ were better when the EM38 was in the horizontal dipole and they greatly improved with increasing depth. In the deeper part of the soils in this vineyard, the correlation achieved *r* values of 0.670 and 0.656 for the horizontal and vertical dipole respectively, but they were not as good as estimations derived for certain chemical and physical components of the soils ($Na^+$, $Mg^{2+}$, clay and sand, see Table 6). The best estimation of $\theta_v$ from the EM38 corresponded to moisture in soil depths measured between 0.60 and 0.90 m using the EM38 values of $EC_a$ detected in the horizontal dipole ($EC_a1h$) mode (Table 5).

## Relationship between $EC_a$ and chemical and physical soil properties

The *r* values between weighted values of the soil analyses (Eq. 1) and soil electrical conductivity measurements were calculated at each field campaign (Table 6). There was a

**Table 5** Pearson Product Moment Correlations ($r$) between $EC_a$ ($mS\ m^{-1}$) and soil volumetric water content (%) for the depths of measurements

| | Depths (m) of $\theta_v$ measurement | | | | | | |
|---|---|---|---|---|---|---|---|
| | 0–0.15 | 0.15–0.30 | 0.30–0.45 | 0.45–0.60 | 0.60–0.90 | Mean profile (0–0.90 m) | Weighted average (0–0.90 m) |
| $EC_a1v$ | −0.212 | 0.212 | 0.514** | 0.393** | 0.656** | 0.528** | 0.601** |
| $EC_a1h$ | −0.228 | 0.363* | 0.561** | 0.464** | 0.670** | 0.603** | 0.661** |

Analyses were performed for the overall average of for all depths sampled (mean profile), and the weighted average (Eq. 1) inasmuch as each sample depth was different (weighted average)

Correlations were significant at * $p \leq 0.05$ or at ** $p \leq 0.01$

**Table 6** Pearson product moment correlations ($r$) between soil chemical and physical soil properties and $EC_a$ for the three field campaigns

| | July 8th | | July 29th | | September 19th | |
|---|---|---|---|---|---|---|
| | Horizontal ($EC_a1h$) | Vertical ($EC_a1v$) | Horizontal ($EC_a2h$) | Vertical ($EC_a2v$) | Horizontal ($EC_a3h$) | Vertical ($EC_a3v$) |
| $K^+$ | 0.069 | 0.232 | 0.046 | 0.057 | 0.017 | 0.038 |
| $Na^+$ | 0.679** | 0.797** | 0.800** | 0.878** | 0.804** | 0.808** |
| $Ca^{2+}$ | 0.523** | 0.442** | 0.459** | 0.356* | 0.293 | 0.241 |
| $Mg^{2+}$ | 0.677** | 0.667** | 0.702** | 0.744** | 0.721** | 0.665** |
| Sand | −0.701** | −0.716** | −0.731** | −0.719** | −0.622** | −0.570** |
| Silt | 0.473** | 0.475** | 0.523** | 0.467** | 0.367* | 0.336* |
| Clay | 0.755** | 0.778** | 0.765** | 0.788** | 0.692** | 0.652** |

Correlations were significant at * $p \leq 0.05$ or at ** $p \leq 0.01$

high correlation between $EC_a$ and the soil particle size distribution (sand and clay). The correlation coefficient between $EC_a$ and sand varied between −0.622 and −0.731, while the correlations with clay content, in turn, ranged from 0.652 to 0.788 (Table 6). The data overall suggested that $EC_a$ was associated to a large extent with electrolyte (cation) concentration, as opposed to particle size. This is in general agreement with the report of Shmulik (2005). Larger particle sizes were generally associated with a modest decrease in electrical conductivity of soil.

The correlations were highest when considering the relation between soil $Na^+$ and $Mg^{2+}$ and $EC_a$, which may suggest that these are more strongly associated with electrical properties of this soil. Correlations between $EC_a$ and soil extractable calcium ($Ca^{2+}$) content were nonetheless statistically significant with the exception of the measurements made on the 29th of September. Surprisingly, no relation emerged between $EC_a$ and extractable potassium contents of these soils (Table 6).

## Linear regression estimates for $EC_a$ and soil chemical and physical properties

One objective of this investigation was to develop regression models for those edaphic factors associated with $EC_a$ that are important to viticulture practices. From these analyses

**Table 7** Linear regression coefficients ($r^2$) between $EC_a$ and $Na^+$, $Mg^{2+}$, clay and sand soil contents for the three field campaigns (RMSE in parentheses)

| | July 8th | | July 29th | | September 19th | |
|---|---|---|---|---|---|---|
| | Horizontal ($EC_a1h$) | Vertical ($EC_a1v$) | Horizontal ($EC_a2h$) | Vertical ($EC_a2v$) | Horizontal ($EC_a3h$) | Vertical ($EC_a3v$) |
| $Na^+$ | 0.460 (0.43) | 0.636 (0.35) | 0.639 (0.35) | 0.770 (0.28) | 0.647 (0.35) | 0.653 (0.34) |
| $Mg^{2+}$ | 0.459 (2.16) | 0.445 (2.18) | 0.493 (2.09) | 0.554 (1.96) | 0.520 (2.14) | 0.442 (2.17) |
| Clay | 0.569 (4.82) | 0.605 (4.62) | 0.586 (4.73) | 0.621 (4.52) | 0.478 (8.16) | 0.426 (5.54) |
| Sand | 0.491 (8.23) | 0.513 (8.04) | 0.534 (7.87) | 0.517 (8.01) | 0.387 (4.87) | 0.325 (9.47) |

and under the conditions of measurement, it was apparent that $EC_a$ measurements and thematic mapping were appropriate in this field for mapping predicted spatial distributions of clay, sand, $Na^+$ and $Mg^{2+}$, all of which are important in the cultivation of grape. Thus, with the exception of potassium, $EC_a$ did provide a useful proxy for such soil properties.

Linear models between $Na^+$, $Mg^{2+}$, clay and sand soil contents with $EC_a$ reports from each field campaign were computed (Table 7). Differences in linear regression fits are probably due to differences in environmental conditions between the three dates of campaign. Studies have verified that soil moisture content (Sudduth et al. 2001) and

**Table 8** Comparison of the linear regression coefficient ($r^2$) between $Na^+$ content and $EC_a$ for the three field campaigns (July 8th, July 29th and September 19th, 2005) for horizontal ($EC_a1h$, $EC_a2h$ and $EC_a3h$) and vertical ($EC_a1v$, $EC_a2v$ and $EC_a3v$) dipole orientations

| Soil factor | Model | Reduced model | | | Full model | | | n | F- value | Prob > F | Sig. |
|---|---|---|---|---|---|---|---|---|---|---|---|
| | | $SSE_R$ | $df_R$ | $MSE_R$ | $SSE_F$ | $df_F$ | $MSE_F$ | | | | |
| $Na^+$ | Combined | 46.920 | 252 | 0.186 | 30.750 | 242 | 0.127 | 254 | 12.720 | 0.000 | ** |
| $Na^+$ | horizontal-vertical | 46.920 | 252 | 0.186 | 41.560 | 250 | 0.166 | 254 | 16.110 | 0.000 | ** |
| $Na^+$ | $EC_a1v$-$EC_a1h$ | 14.540 | 84 | 0.173 | 12.860 | 82 | 0.157 | 86 | 5.372 | 0.006 | ** |
| $Na^+$ | $EC_a2v$-$EC_a2h$ | 14.030 | 84 | 0.167 | 8.400 | 82 | 0.102 | 86 | 27.523 | 0.000 | ** |
| $Na^+$ | $EC_a3v$-$EC_a3h$ | 11.580 | 80 | 0.145 | 9.500 | 78 | 0.122 | 82 | 8.573 | 0.000 | ** |
| $Na^+$ | $EC_a1v$-$EC_a2v$ | 9.609 | 84 | 0.114 | 8.451 | 82 | 0.103 | 86 | 5.618 | 0.005 | ** |
| $Na^+$ | $EC_a1v$-$EC_a3v$ | 13.755 | 85 | 0.162 | 10.148 | 83 | 0.122 | 87 | 14.752 | 0.000 | ** |
| $Na^+$ | $EC_a2v$-$EC_a3v$ | 10.359 | 85 | 0.122 | 8.231 | 83 | 0.099 | 87 | 10.733 | 0.000 | ** |
| $Na^+$ | $EC_a1h$-$EC_a2h$ | 16.266 | 84 | 0.194 | 12.805 | 82 | 0.156 | 86 | 11.081 | 0.000 | ** |
| $Na^+$ | $EC_a1h$-$EC_a3h$ | 16.612 | 79 | 0.210 | 12.206 | 77 | 0.159 | 81 | 13.895 | 0.000 | ** |
| $Na^+$ | $EC_a2h$-$EC_a3h$ | 9.774 | 79 | 0.124 | 9.662 | 77 | 0.125 | 81 | 0.445 | 0.642 | |
| $Mg^{2+}$ | Combined | 1435.774 | 252 | 5.698 | 1110.799 | 242 | 4.590 | 254 | 7.080 | 0.000 | ** |
| $Mg^{2+}$ | horizontal-vertical | 1435.774 | 252 | 5.698 | 1318.704 | 250 | 5.275 | 254 | 11.097 | 0.000 | ** |
| Clay | Combined | 8129.545 | 252 | 32.260 | 5863.618 | 242 | 24.230 | 254 | 9.352 | 0.000 | ** |
| Clay | horizontal-vertical | 8129.545 | 252 | 32.260 | 7305.757 | 250 | 29.220 | 254 | 14.095 | 0.000 | ** |
| Sand | Combined | 22018 | 252 | 87.372 | 17173 | 242 | 70.960 | 254 | 6.828 | 0.000 | ** |
| Sand | horizontal-vertical | 22018 | 252 | 87.372 | 20263 | 250 | 81.050 | 254 | 10.826 | 0.000 | ** |

The table also shows summary statistics for $Mg^{2+}$, clay, and sand content temperature of the EM38 (Robinson et al. 2004) influence measurements acquired with this instrument.

Results of the fitting process for full and reduced forms of a linear model with the combined data are shown in Table 8. The *p* value of the *F*-statistic in Eq. 4 was less than 0.01 for all the soil variables. There were therefore differences among the linear models from different measurement dates or sampling positions. Differences were also obtained between vertical and horizontal sampling positions for all soil variables (Table 8).

Since the differences may be caused by as few as two or as many as all of the measurements, *F*-tests were also carried out for each pair of measurement dates and sampling position so that the source of the differences could be identified. Most of the nine possible paired comparisons for each soil variable produced significant *F*-values, suggesting that significantly different linear models are required for the three EM38 field campaigns and the two sampling orientations. A total of 44 model comparisons were carried out, eleven for each of the four soil quantities. Because of the large number, the full set of comparisons is shown only for $Na^+$. Only the comparisons between the full sets of measurements in the horizontal and vertical positions are shown for $Mg^{2+}$, clay and sand. Table 7 contains the information for the best model for each soil component on each data.The *p* values shown in Table 8 represent the comparisonwise error rate, but they provide an indication of the differences in $EC_a$ values among most position and date combinations.

The predictive value of the regression model for $Na^+$ was significantly better when the measurements were made with the instrument in the vertical position (Table 8). The best estimates for $Na^+$, with the EM38 in the vertical and horizontal orientation respectively, were obtained with data of $EC_a$ from the 29th of July ($EC_a$2v) and the 19th of September ($EC_a$3h) (Table 7).

All differences between the full and reduced models for $Mg^{2+}$ were statistically significant with the exception of $EC_a$1v versus $EC_a$2v and $EC_a$2h versus $EC_a$3h (data not shown). For soil clay content, statistically significant differences were also apparent between the reduced and full models with the exception of $EC_a$1v versus $EC_a$2v and $EC_a$2h versus $EC_a$3h (data not shown). The best linear relationships obtained for explaining clay content with $EC_a$, were obtained with data taken on the 29th of July (Table 7).

The comparative statistical analysis of sand content showed that the predictions with relation to $EC_a$ were better than results obtained in the vertical dipole orientation (Table 8) and the $r^2$ values better than were obtained with the measurements conducted on the 29th of July; values of $r^2 = 0.517$ and 0.534, for the vertical and horizontal orientation respectively (Table 7).

Figure 2 shows the best linear models between $EC_a$ (both vertical and horizontal dipole orientation) and $Na^+$, $Mg^{2+}$, clay and sand soil contents, based on the results of the general linear test (Table 6). It is fairly clear from the coefficients of determination obtained in this investigation that the results obtained with the EM38 in the vertical dipole position ($EC_a$v) were better overall than those obtained with the horizontal orientation ($EC_a$h) (Table 8; Fig. 2). The sole exception concerned estimates for sand content. This result can be explained in part by the observation that higher clay content soil horizons were often at depths of greater than 0.60 m and the EM38 electromagnetic field penetrates to a greater depth (1.5 m versus 0.75 m) using the vertical dipole mode.

On the other hand, the estimates derived from data gathered on the 29th of July (Fig. 2) were significantly better than those from the other dates (Table 8). It is believed this is due to the fact that the vineyard had been irrigated immediately prior to the measurement campaign, although since water was applied through drip irrigation, the majority of that water was constrained away from the point of measurement with the EM38. In addition,

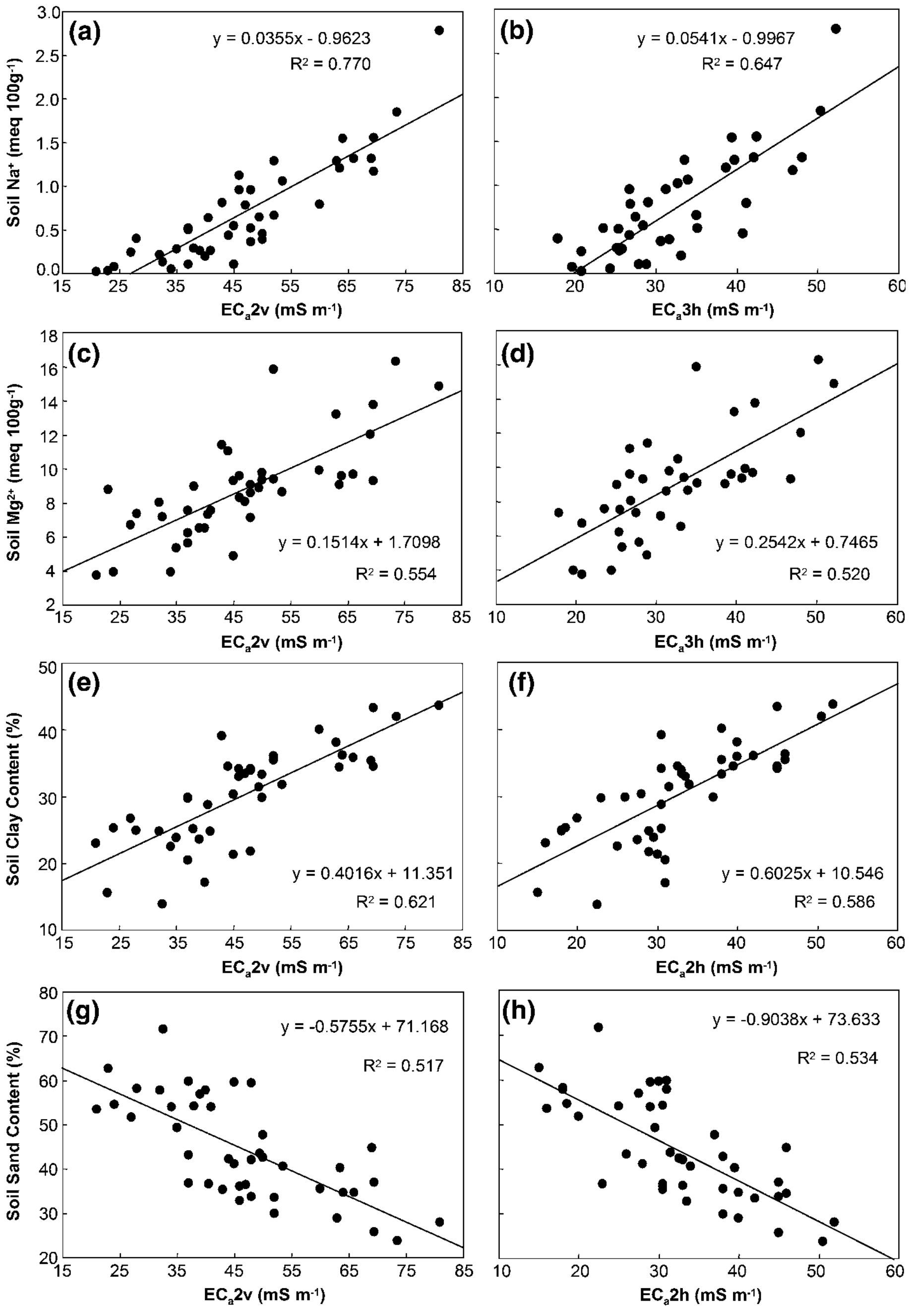


**Fig. 2** Linear relationships between $EC_a$ (mS $m^{-1}$) in vertical dipole orientation (on July 29th, $EC_a2v$) and horizontal dipole orientation (on July 29th, $EC_a2h$ and September 19th $EC_a3h$) and $Na^+$ (meq 100 $g^{-1}$) (**a**, **b**), $Mg^{2+}$ (meq 100 $g^{-1}$) (**c**, **d**), clay (%) (**e**, **f**) and sand (%) (**g**, **h**) soil contents

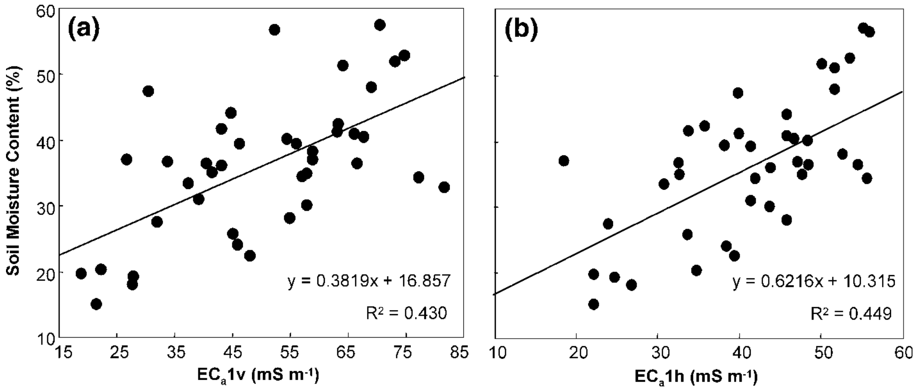


**Fig. 3** Linear relationships between soil moisture content (%, 0.60–0.90 m) and EC$_a$ (mS m$^{-1}$) in the vertical (**a**) and horizontal (**b**) dipole orientations

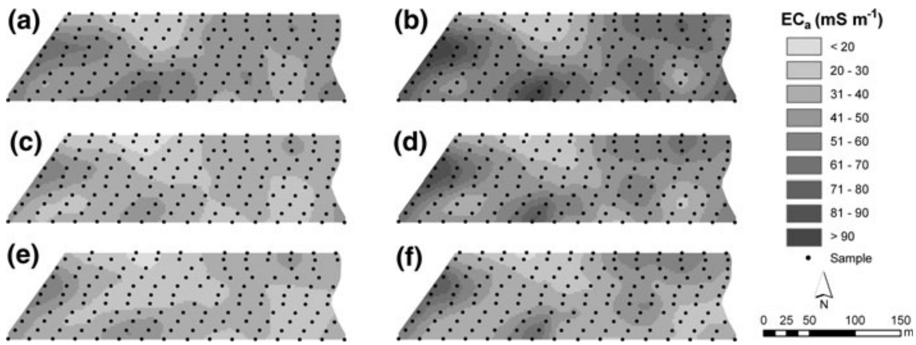


**Fig. 4** Spatial variation of EC$_a$ for the three field campaigns (July 8th, July 29th and September 19th, 2005). EC$_a$ interpolations (mS m$^{-1}$) were obtained by kriging using field samples of EM38 horizontal dipole orientation on July 8th (**a**), July 29th (**c**), September 19th (**e**); and EM38 vertical dipole orientation on July 8th (**b**), July 29th (**d**), September 19th (**f**)

correlations between apparent electrical conductivity and soil moisture were not as good (Fig. 3).

## Spatial distribution of soil variables

Interpolated maps were obtained from the best EC$_a$ linear equations represented in Fig. 2. For maps describing soil variables, all 150 EC$_a$ site locations were employed; unlike the statistical analyses of relational data, in which only the 44 locations coinciding with the soil samples taken to specific depths were used.

The EC$_a$ data gathered from the vertical and horizontal dipole measurements yielded maps that permitted the direct observation of patterns of spatial variability (Fig. 4). Maps of EC$_a$ indicated the distribution of differences in dielectric constant over the vineyard and reveal that the measurements were similar during each of the field campaigns (Fig. 4). Nonetheless, best results were obtained using EM38 data measured on July 29th for soil

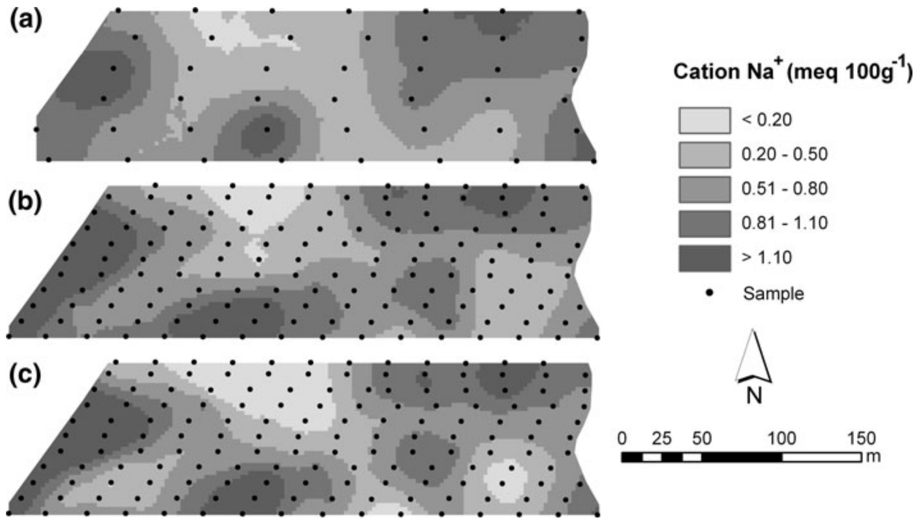


**Fig. 5** Spatial distribution of extractable soil $Na^+$ content (meq 100 $g^{-1}$). Maps obtained by kriging using soil analytical data (**a**), and field samples of EM38 horizontal dipole on September 19th (**b**) and EM38 vertical dipole on July 29th (**c**)

$Na^+$ and $Mg^{2+}$ concentration in the vertical positioning (Table 7) while, for sand and clay content, best results were achieved on July 29th for the horizontal and vertical dipoles, respectively. Thus, for the following mapping exercises, data is presented for these four parameters ($Na^+$, $Mg^{2+}$, sand and clay) with September 19th (horizontal, $Na^+$ and $Mg^{2+}$) and July 29th (vertical, sand and horizontal, clay) EM38 measurements for comparison.

The spatial distribution of extractable soil $Na^+$ content from soil analytical data measured in the field is shown in Fig. 5a, and from regression models derived from $EC_a3h$ (Fig. 5b) and from $EC_a2v$ (Fig. 5c) measured on September 19th and July 29th respectively. It can be seen that the spatial distribution patterns are very similar, suggesting good estimates can be obtained for extractable $Na^+$ using $EC_a$ with the EM38, although it must be kept in mind that ground verification and calibration will be required in all cases.

The estimation of extractable soil $Mg^{2+}$ content (Fig. 6a) by regression of the $EC_a$ fit reasonably well, especially using $EC_a3h$ (Fig. 6b) and $EC_a2v$ (Fig. 6c) measured on September 19th and July 29th respectively. The variation in soil particle size distribution (texture) using the soils analyses revealed a clear spatial pattern for both clay (Fig. 7a) and sand (Fig. 8b) contents that corresponded well with those of $Na^+$ (Fig. 5a) and $Mg^{2+}$ (Fig. 6a).

Soil moisture content changes were very abrupt in the shallower soil horizons, whereas more gradual changes were noted as deeper soil profiles were encountered by the TDR wave guides (Table 2). For this reason, the thematic maps for soil moisture content were visually different (Fig. 9). In absolute terms, the $\theta_v$ values differ markedly by dipole position (Figs. 9a–c), but in relative terms they are similar. This statement can apply to just about all the well-estimated soil parameters that were modeled ($Na^+$, $Mg^{2+}$, sand and clay), since the relative distribution patterns were similar regardless of dipole orientation (Figs. 5, 6, 7, 8). This indicated that electrical conductivity may be better suited to mapping relative values of soil properties than absolute values.

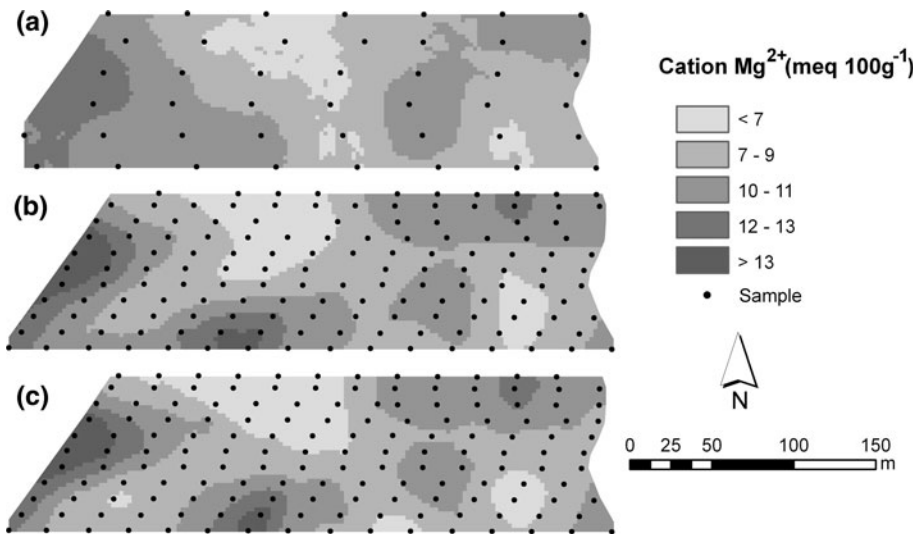


**Fig. 6** Spatial distribution of extractable soil $Mg^{2+}$ content (meq 100 $g^{-1}$). Maps obtained by kriging using soil analytical data (**a**), and field samples of EM38 horizontal dipole on September 19th (**b**) and EM38 vertical dipole on July 29th (**c**)

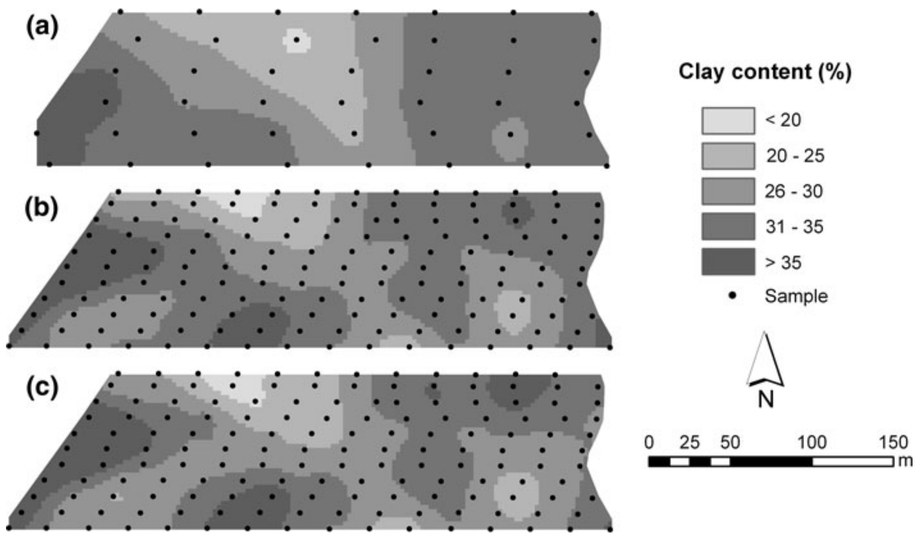


**Fig. 7** Spatial distribution of soil clay content (%). Maps obtained by kriging using soil analytical data (**a**) and field samples of EM38 horizontal dipole on July 29th (**b**) and EM38 vertical dipole on July 29th (**c**)

The findings were similar to those of Johnson et al. (2001), Carroll and Oliver (2005) and Jung et al. (2005) who focused on Midwest soils and factors of nitrogen fertility. They were similar in as much as particle size distribution (sand and clay), which is extremely important in viticulture for estimates of total available water, were highly correlated with $EC_a$. For other chemical and physical properties (such as extractable $K^+$ content), the

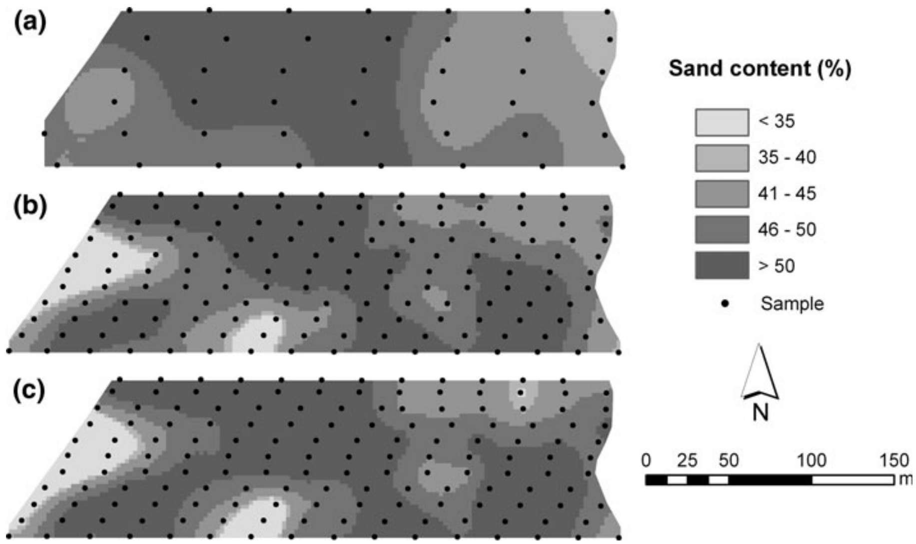


**Fig. 8** Spatial distribution of soil sand content (%). Maps obtained by kriging using soil analytical data (**a**) and field samples of EM38 horizontal dipole on July 29th (**b**) and EM38 vertical dipole on July 29th (**c**)

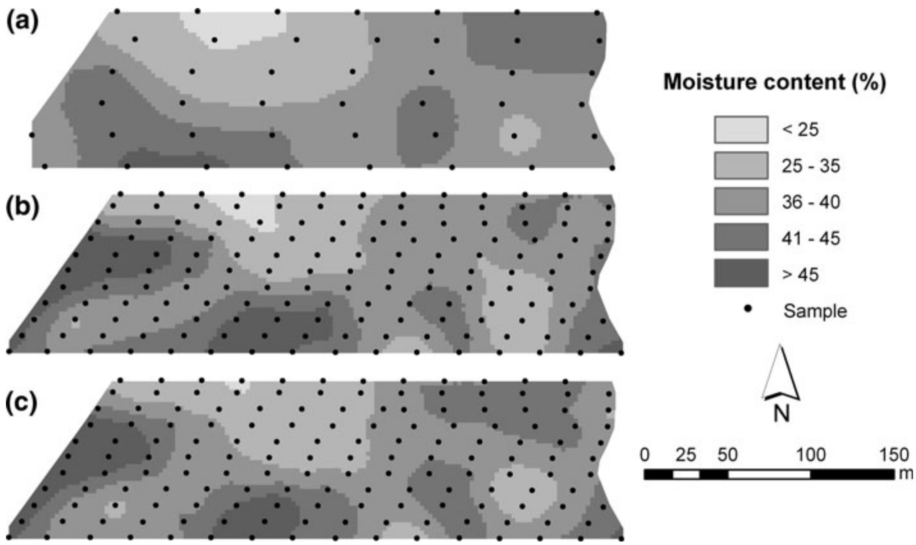


**Fig. 9** Spatial distribution of volumetric soil moisture content ($\theta_v$, 0.60–0.90 m depth). Maps of $\theta_v$ obtained by kriging using field samples of TDR (**a**), EM38 horizontal dipole on July 8th (**b**) and EM38 vertical dipole on July 8th (**c**)

accuracy and precision of the estimates were lower. The above information would be valuable to precision viticulture as it relates to vineyard establishment. As pointed out by Smart et al. (2008), fruit loads are most often managed in viticulture. But vineyard establishment can require decisions such as dividing larger parcels into smaller irrigation blocks, or into blocks where rootstocks that differ in 'vigor' (Bauerle et al. 2008) or drought tolerance are required. The cartographic exercises presented in this report indicated that $EC_a$ can be a useful proxy in this respect.

## Conclusions

Results showed that $EC_a$ data may be used within a GIS framework to obtain a cartographic representation of spatially complex soils. The highest correlation values were obtained with the EM38 in the vertical dipole and no spatial patterns in differences were detected between measurements made in the vertical or horizontal orientation. This investigation indicated that preliminary mapping exercises using $EC_a$ could save time and resources in the evaluation of soil resources that are important with respect to vineyard development and establishment, with the exception of soil depth. The soil components that were most effectively mapped using $EC_a$ were the chemical properties of extractable $Na^+$ and $Mg^{2+}$, while the best estimated physical properties were clay and sand content. These are of considerable importance for grape performance and nutrition.

**Acknowledgements** The authors acknowledge financial support from the Ministerio de Educación y Ciencia (agreement PR2005-0291) and the Consejería de Educación de la Junta de Castilla y León (project LE002B07) of Spain to José R. Rodríguez-Pérez. The John Deere Division of Global Ag Services, USDA Western Viticulture Consortium (agreement 05-34360-15800) and American Vineyard Foundation provided further financial support to David R. Smart and Jean-Jacques Lambert.



## References

Acevedo-Opazo, C., Tisseyre, B., Guillaume, S., & Ojeda, H. (2008). The potential of high spatial resolution information to define within-vineyard zones related to vine water status. *Journal of Precision Agriculture, 9*, 285–302.

Allred, B. J., Daniels, J. J., & Ehsani, M. R. (2008). *Handbook of agricultural geophysics*. Boca Raton, FL, USA: CRC Press.

Bates, D. M., & Watts, D. G. (1988). *Nonlinear regression analysis and its applications*. New York: John Wiley and Sons.

Bauerle, T., Smart, D. R., Bauerle, W., Stockert, C. M., & Eissenstat, D. M. (2008). Root foraging in response to heterogeneous soil moisture in two grapevines that differ in potential growth rate. *New Phytologist, 179*, 857–866.

Bramley, R. G. V. (2003). Precision viticulture—tools to optimize winegrape production in a difficult landscape. In: P. Robert (Ed.), *Proceedings of the 6th international conference on precision agriculture and other precision resources management* (pp. 648–657, CDROM). Madison, WI, USA: ASA-CSA-SSSA.

Bramley, R. G. V. (2004). Understanding variability in winegrape production systems. 2 Within vineyard variation in yield over several vintages. *Australian Journal of Grape and Wine Research, 11*, 33–44.

Bramley, R. G. V., & Hamilton, R. P. (2004). Understanding variability in winegrape production systems. 1 Within vineyard variation in yield over several vintages. *Australian Journal of Grape and Wine Research, 10*, 32–45.

Bramley, R. G. V., & Lanyon, D. M. (2002). Evidence in support of the view that vineyards are leaky–Indirect evidence and food for thought from precision viticulture research. In R. G. V. Bramley & D. M. Lanyon (Eds.), *Vineyard 'leakiness', final report on GWRDC project No. GWR01/04* (pp. 31–37). Adelaide, Australia: CSIRO Land and Water/Grape and Wine Research and Development Corporation.

Carroll, Z. L., & Oliver, M. A. (2005). Exploring the spatial relations between soil physical properties and apparent electrical conductivity. *Geoderma, 128*, 354–374.

Corwin, D. L., & Lesch, S. M. (2005). Apparent soil electrical conductivity measurements in agriculture. *Computers and Electronics in Agriculture, 46*, 11–43.

De Clercq, W. P., & Van Meirvenne, T. M. (2005). Effect of long-term irrigation application on the variation of soil electrical conductivity in vineyards. *Geoderma, 128*, 133–211.

Domsch, H., & Giebel, A. (2004). Estimation of soil textural features from soil electrical conductivity recorded using the EM38. *Precision Agriculture, 5*, 389–409.

ESI. (2002). *MoisturePoint$^{TM}$. Technical paper. MP-917 Technical Brief 1*. Environmental Sensors Inc. http://www.esica.com/_docs/tb01.pdf. Accessed 17 December 2010.

Gardner, W. H. (1986). Water Content. In G. S. Campbell, R. D. Jackson, M. M. Mortland, D. R. Nielsen, & A. Klute (Eds.), *Methods of soil analysis: Part I—physical and mineralogical methods* (pp. 493–541). Madison, WI, USA: American Society of Agronomy.

Gee, G. W., & Bauder, J. W. (1986). Particle-size Analysis. In G. S. Campbell, R. D. Jackson, M. M. Mortland, D. R. Nielsen, & A. Klute (Eds.), *Methods of soil analysis: Part I—physical and mineralogical methods* (pp. 383–411). Madison, WI, USA: American Society of Agronomy.

Geonics Limited. (1999). *EM38 ground conductivity meter—operating manual*. Mississauga, Ontario, Canada

Hedley, C. B., Yule, I. J., Eastwood, C. R., Shepherd, T. G., & Arnold, G. (2004). Rapid identification of soil textural and management zones using electromagnetic induction sensing of soils. *Australian Journals of Soil Research, 42*, 389–400.

Hendrickx, J. M. H., Borchers, B., Corwin, D. L., Lesch, S. M., Hilgendorf, A. C., & Schlue, J. (2002). Inversion of soil conductivity profiles from electromagnetic induction measurements: Theory and experimental verification. *Soil Science Society of America Journal, 66*, 673–685.

Horney, R. D., Taylor, B., Munk, D. S., Roberts, B. A., Lesch, S. M., & Plant, R. E. (2005). Development of practical site-specific management methods for reclaiming salt-affected soil. *Computers and Electronics in Agriculture, 46*, 379–397.

Johnson, C. K., Doran, J. W., Duke, H. R., Wienhold, B. J., Eskridge, K. M., & Shanahan, J. F. (2001). Field-scale electrical conductivity mapping for delineating soil condition. *Soil Science Society of America Journal, 65*, 1829–1837.

Jung, W. K., Kitchen, N. R., Sudduth, K. A., Kremer, R. J., & Motavalli, P. P. (2005). Relationship of apparent soil electrical conductivity to claypan soil properties. *Soil Science Society of America Journal, 69*, 883–892.

Lamb, D. W., Mitchell, A., & Hyde, H. (2005). Vineyard trellising with steel posts distorts data from EM soil surveys. *Australian Journal of Grape and Wine Research, 11*, 24–32.

McNeill, J. D. (1980a). *Electrical conductivity of soils and rocks. Tech note TN-5* (pp. 5–22). Ontario, Canada: Geonics Ltd. http://www.geonics.com/pdfs/technicalnotes/tn5.pdf. Accessed 17 December 2010.

McNeill, J. D. (1980b). *Electromagnetic terrain conductivity measurement at low induction numbers. Tech note TN-6* (pp. 5–15). Ontario, Canada: Geonics Ltd. http://www.geonics.com/pdfs/technicalnotes/tn6.pdf. Accessed 17 December 2010.

Noborio, K. (2001). Measurement of soil water content and electrical conductivity by time domain reflectometry: A review. *Computers and Electronics in Agriculture, 31*, 213–237.

Pella, E. (1990). *Elemental organic analysis 2 state of the art* (pp. 22–28). USA: American Laboratory.

Robinson, D. A., Lebron, I., Lesch, S. M., & Shouse, P. (2004). Minimizing drift in electrical conductivity measurements in high temperature environments using the EM-38. *Soil Science Society of America Journal, 68*, 339–345.

Sheldrick, B. H. & Wang, C. (1993). Particle-size distribution. In: M. R. Carter (ed.), *Soil sampling and methods of analysis* (pp. 499–511), Ann Arbor (MI, USA): Canadian Society of Soil Science, Lewis Publishers.

Shmulik, P. F. (2005). Soil properties influencing apparent electrical conductivity: A review. *Computers and Electronics in Agriculture, 46*, 45–70.

Smart, D. R., Breazeale, A., Viers, J., & Plant, R. E. (2008). Anthropogenic intervention in shaping terroir in a California Pinot Noir vineyard. In F. Murisier & V. Zufferey (Eds.), *Proceedings of the V*th *international terroir conference*, Nyon Switerland, May 19–23, 2008. Département Fédéral de l'Économie Agroscope Changins-Wädenswil, DFE.

Smart, D. R., Schwass, E., Morano, L., & Lakso, A. L. (2006). Grapevine root distributions: A comprehensive analysis and review. *American Journal of Enology and Viticulture, 57*, 89–104.

Steenwerth, K. L., Drenovsky, R. E., Lambert, J. J., Kluepfel, D. A., Scow, K. M., & Smart, D. R. (2008). Soil morphology, depth and grapevine root frequency influence microbial communities in a Pinot Noir vineyard. *Soil Biology and Biochemistry, 40*, 1330–1340.

Sudduth, K. A., Drummond, S. T., & Kitchen, N. R. (2001). Accuracy issues in electromagnetic induction sensing of soil electrical conductivity for precision agriculture. *Computers and Electronics in Agriculture, 31*, 239–264.

Thomas, G. W. (1982). Exchangeable cations. In A. L. Page et al. (Eds.), *Methods of soil analysis: Part 2. Chemical and microbiological properties* (pp. 159–165). ASA Monograph Number 9.

Topp, G. C., Davis, J. L., & Annan, A. P. (1980). Electromagnetic determination of soil water content: Measurements in coaxial transmission lines. *Water Resources Research, 16*, 574–582.

US Salinity Lab Staff. (1954). pH reading of saturated soil paste. In L. A. Richards (Ed.), *Diagnosis and improvement of saline and alkali soils. USDA agricultural handbook No. 60*. Washington, DC: US Government Printing Office.

Williams, S., & Bramley, R. G. V. (2003). Some tips on data management for precision agriculture. *Precision Agriculture News, 2*, 6–8.

Winkel, T., Rambal, S., & Bariac, T. (1995). Spatial variation and temporal persistence of grapevine response to a soil texture gradient. *Geoderma, 68*, 67–78.